



Published in final edited form as:

*Neurosci Lett.* 2023 September 25; 814: 137419. doi:10.1016/j.neulet.2023.137419.

## The clinically-approved compounds, pramipexole and dexpramipexole, reverse chronic allodynia from sciatic nerve damage in mice, and alter IL-1 $\beta$ and IL-10 expression from immune cell culture

J.E Sanchez<sup>a</sup>, S Noor<sup>a</sup>, M.S Sun<sup>a</sup>, J Zimmerly<sup>a</sup>, A Pasmay<sup>a</sup>, J.J Sanchez<sup>a</sup>, A.G Vanderwall<sup>a</sup>, MK Haynes<sup>b</sup>, L.A Sklar<sup>b</sup>, P.R Escalona<sup>c,d</sup>, E.D Milligan<sup>a,\*</sup>

<sup>(a)</sup>Department of Neurosciences, School of Medicine, University of New Mexico Health Sciences Center, Albuquerque, NM, 87131, USA.

<sup>(b)</sup>Center for Molecular Discovery (CMD) Innovation, Discovery and Training Complex (IDTC), University of New Mexico Health Sciences Center, Albuquerque, NM, 87131, USA.

<sup>(c)</sup>Department of Psychiatry, School of Medicine, University of New Mexico Health Sciences Center, Albuquerque, NM, 87131, USA.

<sup>(d)</sup>New Mexico VA Health Care System, Albuquerque NM, 87108, USA.

### Abstract

During the onset of neuropathic pain from a variety of etiologies, nociceptors become hypersensitized, releasing neurotransmitters and other factors from centrally-projecting nerve terminals within the dorsal spinal cord. Consequently, glial cells (astrocytes and microglia) in the spinal cord are activated and mediate the release of proinflammatory cytokines that act to enhance pain transmission and sensitize mechanical non-nociceptive fibers which ultimately results in light touch hypersensitivity, clinically observed as allodynia. Pramipexole, a D2/D3 preferring agonist, is FDA-approved for the treatment of Parkinson's disease and demonstrates efficacy in animal models of inflammatory pain. The clinically-approved R(+) enantiomer of pramipexole, dexpramipexole, has reduced D2/D3 agonist actions and is efficacious in animal models of inflammatory and neuropathic pain. The current experiments focus on the application of a mouse model of sciatic nerve neuropathy, chronic constriction injury (CCI), that leads to allodynia

\*Correspondence: E.D. Milligan: EMilligan@salud.unm.edu.

#### Author Contributions

JES, SN, PE, and EM developed the conception and design of the study, and edited the manuscript. MH, LAS and SN generated the *in vitro* experimental design. JES, MSS, SN, collected behavioral data and tissues. SN, MS, JZ and AP processed the tissues and performed protein assays and real-time PCR, and JES, MSS, and ED performed statistical analysis. JES, SN and EM wrote various drafts and contributed to the final the manuscript. All authors contributed to manuscript revision, read, and approved the submitted version

#### Conflict of Interest

The authors declare that the research was conducted in the absence of any commercial or financial relationships that could be construed as a potential conflict of interest.

**Publisher's Disclaimer:** This is a PDF file of an unedited manuscript that has been accepted for publication. As a service to our customers we are providing this early version of the manuscript. The manuscript will undergo copyediting, typesetting, and review of the resulting proof before it is published in its final form. Please note that during the production process errors may be discovered which could affect the content, and all legal disclaimers that apply to the journal pertain

and is previously characterized to generate spinal glial activation with consequent release IL-1 $\beta$ . We hypothesized that both pramipexole and dexpramipexole reverse CCI-induced chronic neuropathy in mice, and in human monocyte cell culture studies (THP-1 cells), pramipexole prevents IL-1 $\beta$  production. Additionally, we hypothesized that in rat primary splenocyte culture, dexpramipexole increases mRNA for the anti-inflammatory and pleiotropic cytokine, interleukin-10 (IL-10). Results show that following intravenous pramipexole or dexpramipexole, a profound decrease in allodynia was observed by 1 hr, with allodynia returning 24 hr post-injection. Pramipexole significantly blunted IL-1 $\beta$  protein production from stimulated human monocytes and dexpramipexole induced elevated IL-10 mRNA expression from rat splenocytes. The data support that clinically-approved compounds like pramipexole and dexpramipexole support their application as anti-inflammatory agents to mitigate chronic neuropathy, and provide a blueprint for future, multifaceted approaches for opioid-independent neuropathic pain treatment.

### Keywords

pramipexole; dexpramipexole; neuropathic pain; neuroimmune; IL-1 $\beta$ ; IL-10

---

### Introduction.

Pramipexole, also known as (–)-pramipexole, is a compound that selectively agonizes the dopamine D2/D3 receptors in the central nervous system (CNS) (Wilson et al. 2020; Mierau et al. 1995) and is characterized with a good safety profile for the long-term treatment of Parkinson's Disease (Edinoff et al. 2020; Hauser et al. 2014) and restless leg syndrome (Gossard et al. 2021; Liu et al. 2016). The therapeutic action of pramipexole extends to pain suppressive actions, as evidenced in human studies and animal models of Parkinson's disease (Cao et al. 2016), fibromyalgia (Carville et al. 2008; Marcus 2009; Martins et al. 2022), inflammatory pain (Santamaria-Anzures et al. 2023; Edwards et al. 2022) and neuropathic pain (Rodgers et al. 2019). Interestingly, pramipexole inhibited the expression of the transcription factor for proinflammatory cytokines, nuclear factor- $\kappa$ B (NF- $\kappa$ B) in the dorsal spinal cord while dose-dependently suppressing mechanical hypersensitivity to non-noxious (i.e., mechanical allodynia) and noxious (mechanical hyperalgesia) touch in mice given hindpaw formalin (Bottero et al. 2003; Santamaria-Anzures et al. 2023).

The activation of the immune receptor, toll like receptor 4 (TLR4), on astrocytes and microglia is triggered by various endogenous cell-stress signaling factors from damaged neurons including nociceptors that leads to intracellular activation of the NF- $\kappa$ B (Andersson, Tracey, and Yang 2021; Kato, Agalave, and Svensson 2016; Donnelly, Chen, and Ji 2020). TLR4-NF- $\kappa$ B actions are responsible for the synthesis of precursor cytokines including pro-IL-1 $\beta$ . Thus, the TLR4-NF- $\kappa$ B-IL-1 $\beta$  pathway mediates immune responses (Ghosh et al. 2006; He, Franchi, and Nunez 2013; O'Neill and Bowie 2007) (Andersson, Tracey, and Yang 2021), including following sensory neuron damage (Donnelly, Chen, and Ji 2020; Kato, Agalave, and Svensson 2016).

Work in animal models of pathological pain from a wide range of etiologies demonstrate that chronic neuropathy develops from sensitized nociceptors and spinal pain projection

neurons due, in part, to activated astrocytes and microglia, the NF- $\kappa$ B - IL-1 $\beta$  signaling pathway in the dorsal horn of the spinal cord (Grace et al. 2021; Sideris-Lampretsas and Malcangio 2021; Kato, Agalave, and Svensson 2016). Recently, pramipexole demonstrated antiallodynic and antihyperalgesic actions in a rat model of peripheral inflammatory pain with concurrent suppression of protein NF $\kappa$ B and IL-1 $\beta$  in the dorsal horn of the spinal cord (Santamaria-Anzures et al. 2023). Pramipexole reduces several inflammatory factors that create edema in a model of local inflammation (Sadeghi et al. 2017), suppresses the TLR4-NF $\kappa$ B-NLRP3 inflammasome pathway in acute pancreatitis (Fawzy et al. 2022), and reduces brain IL-1 $\beta$  in a mouse model of inflammation-induced depression (Lieberknecht et al. 2017). Conversely, interleukin-10 (IL-10) is established to suppress CCI-induced allodynia and pleiotropically control the actions of TLR4-NF- $\kappa$ B as well as a variety of proinflammatory cytokines including IL-1 $\beta$  in immune cells and in the CNS (Donnelly, Dickensheets, and Finbloom 1999; Gonzalez et al. 2009; Greenhill et al. 2014; Moore et al. 2001; Milligan et al. 2005; Milligan et al. 2012; Milligan et al. 2006; Sloane et al. 2004; Vanderwall et al. 2018)

Therefore, the current study explored whether pramipexole could reverse chronic allodynia in a mouse model of sciatic nerve neuropathy, referred to as chronic constriction injury (CCI), which has been well-established in the rat (Bennett and Xie 1988; Dowdall, Robinson, and Meert 2005). The CCI model induces intraneuronal inflammatory edema, focal sciatic nerve ischemia and some degree of Wallerian degeneration due to the loose ligation of absorbable chromic gut suture material; sequelae that result in chronic neuropathy in the rat similar to that observed in human pain patients (Robinson and Meert 2005; Bennett and Xie 1988). The development of allodynia from sciatic CCI is among the observations that is in-common with other rodent models of peripheral neuropathy (Dowdall, Robinson, and Meert 2005). Given nearly 50% of chronic peripheral neuropathies involve inflammatory processes (Cohen, Vase, and Hooten 2021; Vellucci 2012), and the CCI model combines both direct nerve trauma and inflammation, the current study applied CCI in the mouse previously characterized in our laboratory to persist for many weeks (Noor et al. 2019; Wilkerson et al. 2020; Wilkerson et al. 2022).

Dexpramipexole, the R(+) enantiomer of pramipexole, is a weak dopamine D2/D3 receptor agonist (Gribkoff and Bozik 2008; Schneider and Mierau 1987). Given that dopamine itself can activate D2/D3 on normal human leukocytes triggering proinflammatory cytokine release (Besser, Ganor, and Levite 2005), dexpramipexole was chosen to compare against pramipexole's anti-inflammatory actions as a therapeutic with reduced D2/D3 actions. Dexpramipexole is highly orally bioavailable, water-soluble, and rapidly achieves and maintains high CNS concentrations relative to plasma (Cudkowicz et al. 2011). In clinical development for the treatment of amyotrophic lateral sclerosis, dexpramipexole is well tolerated with a high safety profile demonstrated in a Phase 3 clinical trial (Cudkowicz et al. 2013). Recently, dexpramipexole treatment resulted in anti-allodynic actions of CCI-nerve damage in mice and blocked TTX-resistant sodium conductances in cultured rat sensory neurons, with selectivity for the voltage-gated sodium channel (Nav) 1.8 (Urru et al. 2020). Together, these reports suggest dexpramipexole exerts pleiotropic pain-suppressive actions.

Utilizing the neuropathic rodent model, CCI, the goals of the current study aimed to determine whether (–)-pramipexole and its enantiomer, dexpramipexole ((+)-pramipexole) reverse sciatic nerve CCI-induced chronic allodynia in mice. Additionally, cell culture studies were performed to determine whether; (1) pramipexole prevents protein IL-1 $\beta$  production in TLR4-NF $\kappa$ B stimulated human leukocytes using cultured THP-1 cells, which are an ideal human monocyte cell line characterized with high TLR4 expression and activation with resultant IL-1 $\beta$  production (Jakopin and Corsini 2019; Lin et al. 2017), and (2) dexpramipexole increases transcriptional expression of the anti-inflammatory cytokine, IL-10, *ex vivo* in LPS stimulated rat leukocytes derived from the spleen.

## Materials and Methods.

### Animals

The current report utilized adult (10–16 wk) male (N=24 for pramipexole treatment) and female (N=20 for dexpramipexole treatment) C57BL/6 mice (wildtype; FFID: IMSR\_JAX:000664) purchased from Jackson Laboratories (Bar Harbor, ME, USA), at ~20 g and used for *in vivo* application of pramipexole and dexpramipexole, respectively. A total of 9 female ~500 g Long-Evans rats bred in-house with dams purchased from Harlan (Harlan Industries, Indianapolis, IN, USA) were used for the leukocyte cell culture experiment. Male mice were examined for pramipexole's effects on allodynia to be consistent with prior work demonstrating pramipexole's anti-inflammatory and anti-oxidant mechanisms in male inflammatory pain and pancreatitis models (Edwards et al. 2022; Fawzy et al. 2022; Sadeghi et al. 2017). Female mice were applied to examine the effects of dexpramipexole on allodynia to provide sex-complementary data to prior reports that demonstrate dexpramipexole's actions in generating analgesia in male nociceptive and neuropathic pain mouse models (Urru et al. 2020), and its protective effects on neurons in a cell culture model of small fiber neuropathy (Lee et al. 2020). Given sex differences in neuroimmune mechanisms that underlie neuropathy have been reported (Sorge et al. 2015), examining the impact of dexpramipexole as a therapeutic to reverse allodynia in female mice would provide further insight into the potential clinical breadth of applying this compound for neuropathic pain states. All animals were maintained on a standard 12:12 light/dark cycle (lights on from 0600 hrs to 1800 hrs) in a temperature-controlled environment ( $23^{\circ} \pm 2^{\circ}\text{C}$ ) for the duration of the study. Additionally, mice were housed in groups of 4–5 mice/cage, and rats were housed 2–3/cage. All mice were routinely monitored by the animal care staff under the direction of the institutional veterinarian, fed standard rodent chow and water *ad libitum*, with cages and bedding changed every 7 days. All procedures were approved by the Institutional Animal Care and Use Committee (IACUC) of the University of New Mexico Health Sciences Center, conducted in accordance to the NIH Guidelines for the Care and Use of Laboratory Animals, and closely adhered to guidelines from the International Association for the Study of Pain for the use of animals in research (Foundation for Biomedical Research, The Biomedical Investigator's Handbook for Researchers Using Animal Models. Washington, D.C.: FBR, 1987. WWW: <http://www.fbresearch.org/>).

### Chronic constriction injury (CCI)

This study utilized a modified version of a well-established rat peripheral nerve injury model in which pathological sensitivity to light touch, clinically termed allodynia, is induced through a chronic constriction injury (CCI) (Bennett and Xie 1988). Introducing minor modifications to the Bennett and Xie rat model of neuropathic pain has demonstrated the ability to replicate this model of neuropathic pain in mice (Liu et al. 2017; Martucci et al. 2008; Vanderwall et al. 2017; Wilkerson et al. 2020). Under isoflurane anesthesia (1.5–2.0% volume in oxygen, 2.0 l/min), the dorsal left thigh was shaved and cleaned using 70% Ethanol (EtOH) that was air dried prior to surgery. Utilizing a small incision over the posterior thigh, remaining 3 cm below the femur bone, from hip bone to the patella, the muscle fascia of the mouse was exposed. Using aseptic procedures, a blunt dissection was performed to carefully isolate the sciatic nerve by separating the overlying muscular fascia. Sterile plastic probes were then used to locate and lift the sciatic nerve from its pocket within the muscle tissue. Mice were then subjected to unilateral loose ligation of the sciatic nerve with three, 5–0 chromic gut sutures (Ethicon; Somerville, NJ, Cat#634G) performed identically as previously detailed (Noor et al. 2019). While sutures were snugly tied around the sciatic nerve proximal to the trifurcation, pinching was avoided. Throughout the duration of the surgery, sterile 0.9% isotonic saline (Hospira; Cat# NDC 0409-4888-03) was irrigated over the sciatic nerve to prevent dehydration. Sham surgery followed the same surgical procedure but without ligation. The sciatic nerve was gently placed back into position using sterile plastic probes, and the overlying muscle fascia was closed using one 4–0 sterile silk suture (Ethicon; Somerville, NJ, Cat#83G). Wound clips (Kent Scientific Corp.; Cat#INS750344) were utilized to seal the incision closed. Mice fully recovered from anesthesia within approximately 10 min and were monitored daily for post-operative complications such as infection and/or irritation, additionally wound clips were removed approximately 5 days post-surgery. Body weight was monitored prior to and after surgery. Half of the mice were randomly assigned to either sham or CCI surgery. All mice in this study recovered completely from the surgery, without any abnormalities, and remained in the study.

### Behavioral assessment of allodynia

Following a 14-day acclimation to the animal colony room, male, and separately, female mice were subjected to a habituation period. The testing environment is located in same mouse colony room at the opposite wall where to home cages are positioned. The habituation period included placing the mice atop a testing rack within the first 4 hrs of the light cycle (lights on from 0600 hrs to 1800 hrs) in a sound and temperature ( $23^{\circ} \pm 2^{\circ}\text{C}$ ) controlled environment, allowing full access to the plantar hindpaw. Mice were exposed to 4 separate habituation periods for approximately 45 min/day. Sensitivity to mechanical light touch, clinically termed allodynia, was assessed using the von Frey behavioral assay in which calibrated monofilaments (touch-test sensory evaluator: North Coast Medical; Cat# NC12775) were applied to the hindpaw to elicit a paw withdraw response. Hindpaw threshold responses to light mechanical stimuli were assessed by adopting principles of the von Frey fiber test originally developed for the rat (Bonin, Bories, and De Koninck 2014; Chaplan et al. 1994; Milligan et al. 2000; Sommer and Schafers 1998) and modified for the mouse, as previously described (Vanderwall et al. 2018; Wilkerson et al. 2020; Wilkerson

et al. 2022). Briefly, the von Frey behavioral assay using nine calibrated monofilaments (touch-test sensory evaluator: North Coast Medical; Cat#NC12775) were applied to the plantar surface of the left and right hindpaws with laterality applied in random order. A maximum of 3.0 seconds (s) touch stimuli was applied, with repeated stimulus presentations to a single animal using a minimum inter-trial stimulus interval of 30 s. The log intensity of the nine monofilaments used is defined as  $\log_{10}$  (grams  $\times$  10,000) with the range of intensity being as follows reported in log (grams): 2.36 (0.022g), 2.44 (0.028g), 2.83 (0.068g), 3.22 (0.166g), 3.61 (0.407g), 3.84 (0.692g), 4.08 (1.202g), 4.17 (1.479g), and 4.31 (2.042g). Testing was initiated with fiber 3.22 (middle of the assay scale) with subsequent monofilaments used based on the response/non-response of the mouse to the previous monofilament tested. If no response was elicited by the stimulus presented from the 3.22 monofilament, the next “greater” monofilament was tested (e.g., 3.61). If a response was elicited by the stimulus presented from the 3.22 monofilament, the next “lighter” monofilament was tested (e.g., 2.83). A maximum total of six stimulus presentations were applied to each paw. The total number of positive and negative responses were then entered into the computer software program, PsychoFit (<http://psych.colorado.edu/~lharvey>; RRID: SCR\_015381) to determine the absolute withdrawal threshold (50% paw withdrawal threshold), as previously described (Vanderwall et al. 2018). The PsychoFit program fits a Gaussian integral psychometric function to the observed withdrawal rates for each monofilament using a maximum-likelihood fitting method (Milligan et al. 2000), which calculates the 50% paw-withdraw threshold (absolute threshold) that is expressed as absolute  $\log_{10}$  stimulus intensity in (mg  $\times$  10), or stimulus intensity (grams) on a linear scale. Data were plotted using GraphPad Prism. Hindpaw assessment of mice occurred in groups of 4–6 per testing trial. Behavioral assessment was conducted at baseline (BL), at days 3, 7, and Day 10 post-surgery and immediately prior to either pramipexole or dexpramipexole treatment. After pramipexole injection, behavior was reassessed at 1–3, 24, 48, and 72 hrs. After dexpramipexole injection, behavior was reassessed at 1–2, 24–48 hrs post-injection. Time points were chosen to tease apart minimal differences between groups at key times while avoiding overstimulation.

### Drug preparation

**Pramipexole dihydrochloride (Px).**—[(–)-2-amino-4,5,6,7-tetrahydro-6-D-propylamino-benzothiazole dihydrochloride] (Sigma-Aldrich; CAS#:104632-25-9) was initially reconstituted in sterile 0.9% isotonic saline (Hospira; Cat#NDC 0409-4888-03) as a 1 $\mu$ g/ $\mu$ l stock solution, with 100  $\mu$ l aliquots stored in sterile 0.5 ml Eppendorf tubes sealed with parafilm and frozen at –80°C for later use. To identify low but efficacious dose that could exert anti-allodynic efficacy relevant to immune cell activation, a small pilot study with mice (N=2–3) was conducted using a dose that was ten-fold greater from that used in a human monocyte-derived osteoclast cell culture (0.5  $\mu$ g) study (Hanami et al. 2013). Using this dose as initial guidance was examined the lower dose of 0.5  $\mu$ g in mice alongside the small pilot cohort. On the day of injection, aliquots were allowed to thaw at room temperature for 15 minutes, and diluted to 0.1  $\mu$ g/ $\mu$ l or 0.01  $\mu$ g/ $\mu$ l using sterile 0.9% isotonic saline and vortexed for approximately 15s. The volume of each intravenous (i.v.) injection was held constant at 50  $\mu$ l. The vehicle (50  $\mu$ l) for pramipexole consisted solely of sterile

0.9% isotonic saline. Animals were injected within an hour of drug preparation. Half of the mice were randomly assigned to either vehicle or pramipexole.

**Dexpramipexole (DPX).**—The (+)-enantiomer of pramipexole ((R)-pramipexole), [4,5,6,7-tetrahydro-N6-propyl-2,6-benzothiazole-diamine hydrochloride] (Cayman Chemical; Cat#18234) was reconstituted in dimethyl sulfoxide (DMSO) at 5 µg/µl, aliquoted at 10 µl in sterile 0.5 ml Eppendorf tubes sealed with parafilm and frozen at –80°C for later use. The selected dose of 0.5 µg was intended to make comparisons against an equal efficacious dose of pramipexole. On the day of the injection, aliquots were brought to room temperature for 15 minutes, and diluted to 0.5 µg/50 µl using sterile water and vortexed for approximately 15s. The volume of each i.v. injection was held constant at 50 µl containing 10% DMSO. The vehicle consisted of 10% DMSO in sterile water; 50 µl, for DPX. Animals were injected within an hr of drug preparation. Half of the mice were randomly assigned to either vehicle or dexpramipexole.

### Intravenous injection (i.v.)

Pramipexole (Px) [(–)-pramipexole], dexpramipexole (DPX) [(+)-pramipexole], or equivolume vehicle was injected into mouse tail veins on Day 10 post-surgery within 2.5 hours of the initiation of the light cycle. The sham- or CCI-operated mice were given either vehicle or drug (either pramipexole or dexpramipexole). Thus, the experimental design for each drug separately (either pramipexole or dexpramipexole) was a 2 (sham vs. CCI) × 2 (vehicle vs. drug) with N=5–6 in each experimental condition. Intravenous administration was chosen to optimize time of drug uptake and distribution for CNS penetration, which is the site of desired action of these drugs. Sham-operated mice received drug to ensure that the drug itself does not exert effects on hindpaw sensitivity, thereby confounding the interpretation of the effects of either drug. Using aseptic procedures, 50 µl of pramipexole, dexpramipexole or vehicle was collected into individual 1 cc, 27G5/8 insulin syringes (Becton Dickinson; Cat# 329412). Weights of the mice were recorded prior to injection (~20g), followed by placing mouse tails under a heat lamp to dilate the lateral tail vein, providing easier access to the vein. To safely heat the mouse tail without excessively heating the body, the tail was held firmly in place while a soft cloth was placed over the mouse body, leaving the tail exposed and the body shielded from heat. The mouse was then immediately moved to a plastic restraint which contained a slit through the middle, in which the tail is carefully moved through, allowing isolation and proper positioning of the tail for injection. With the tail held firmly in place the needle was then inserted into the lateral tail vein, followed by a small amount of blood efflux into the syringe with a subsequent 10s injection. Following injection, sterile gauze was placed over the point of puncture utilizing a small amount of pressure to prevent excess bleeding. The mouse was then placed back in its home cage and for the following 5–10 min was monitored for any abnormal behavior or adverse side effects of injection. The total time required for handling and injection was approximately 2–3 min, with no need for anesthetics.

### THP-1 cell culture and differentiation

To induce TLR4-NLRP3 inflammasome activation and subsequent IL-1β production, the human monocytic leukemia cell line, THP-1 cells, were primed with lipopolysaccharide

(LPS) (Lin et al. 2017). LPS is made up of cell wall particles from gram-negative bacteria that is highly immunogenic to a variety of immune cells such as monocytes that express TLR4. LPS is a widely used immune activator (Aurell, Hawley, and Wistrom 1999; Hitchins and Merritt 1999; Wei et al. 2007). THP-1 human acute monocytic leukemia cells were obtained from American Type Culture Collection (Manassas, VA, USA). THP-1 cells were grown in complete RPMI (ATCC modified RPMI and supplemented with 10% fetal calf serum and 1% antibiotics). Cells were maintained at  $0.5-1 \times 10^6$  cells/ml in a humidified chamber at 37°C, in a mixture of 95% air and 5% CO<sub>2</sub>. RPMI/ATCC modified media was purchased from ThermoFisher Scientific, MA, USA (catalog# A1049101). Fetal calf serum (#97068-085) and Pen/Strep antibiotics (#450000-652) were purchased from VWR, PA, USA.

On the day of the experiment for detection of IL-1 $\beta$  protein levels, cells were collected by centrifugation and suspended at  $2.5 \times 10^6$  cells/ml; 20  $\mu$ l of cells were plated in sets of three into individual wells, with each set consisting of biological triplicates, using a 384 well tissue culture plate (Greiner, catalog #781280). Conditions were represented in sets of 3 units (wells), with each unit consisting of an average of biological triplicates (thus, 9 wells/condition). Stock solution of LPS (Millipore Sigma, catalog #L2630, 5 mg/ml) was diluted in complete medium to prepare a 200 ng/ml solution (2x solution). Control (complete RPMI media only) or LPS in 25  $\mu$ l volumes was added to respective wells containing 20  $\mu$ l of complete RPMI media resulting in a 45  $\mu$ l well volume to allow for the addition of 5  $\mu$ l stock pramipexole in the subsequent step. Pramipexole stock solution (1  $\mu$ g/ $\mu$ l) was thawed on ice and was first diluted to 10x concentrations (5 ng/ml or 50 pg/ml). A total of 5  $\mu$ l of the stock pramipexole was added to the wells containing 45  $\mu$ l of the previously prepared RPMI media (with or without LPS), resulting in a further 1:10 dilution with a final pramipexole concentration in each well of 500 pg/ml or 5 pg/ml. We chose lower doses than that examined in vivo to account for the lack of drug metabolism occurring in a highly controlled cell culture system with the goal of identifying efficacy at low doses and to avoid spurious effects at exceptionally high doses. 5  $\mu$ l of pramipexole or complete medium was added to respective wells. The plate was placed on a plate shaker for 60 sec for mixing. Cells were then incubated overnight (20 hrs) and cell supernatant samples were used for detecting IL-1 $\beta$  protein levels, detailed below.

### IL-1 $\beta$ detection from THP-1 cells

Culture supernatants from THP-1 cells were assayed for the presence of IL-1 $\beta$  using the MultiCyt<sup>®</sup> QBeads<sup>®</sup> Human PlexScreen Secreted Protein Assay Kit (Intellicyte, NM, USA). The assay was performed according to the manufacturer's instructions. Using a similar principle as sandwich ELISA, QBeads<sup>®</sup> technology allowed faster quantitative measurement of IL-1 $\beta$  levels from fresh supernatant samples. Briefly, following LPS and pramipexole treatments, supernatants were harvested from individual wells and placed in 384 well assay plates (Eppendorf twin.tec PCR plates) and analyzed immediately. Samples were added to wells containing the IL-1 $\beta$  capture beads (beads coated with antibodies against IL-1 $\beta$ ) in appropriate buffer provided with the kit and were incubated at room temperature with rotation. Fluorescent detection antibodies were then added and the assay plate was incubated for an additional 2 hr at room temperature, protected from light with rotation. This allows



the fluorescent signal to be associated with the “capture antibody-IL-1 $\beta$  complex”, with the intensity of the fluorescence directly correlating to the quantity of bound IL-1 $\beta$ . A blank control (media only) and different dilutions of IL-1 $\beta$  standards (lyophilized standards were provided by the kit) were run in parallel to ensure the detection parameters for the unknown samples falls within the range of the standards. A plate shaker was used in each step to ensure thorough mixing. After the incubation steps were completed, plates were sampled using the HyperCyt™ high throughput flow cytometry platform.

The HyperCyt™ instrument consists of an autosampler (e.g., Gilson Gx-274), a peristaltic pump (Gilson Minipuls 3), tubing, and an inlet probe that connects to a compatible flow cytometer. These studies used an Accuri C6. The associated software includes HyperSip™ which controls the autosampler and is used to compose microtiter plate templates, and HyperView™ which is used to bin the time-resolved data files stored in flow cytometry standard 2.0 or 3.0 formats. The platform is set up as described (Edwards et al. 2006).

### Peripheral immune cell stimulation

To complement existing reports examining the effect of dexpramipexole on sensory neuron cultures from the rat (Urru et al. 2020), splenocytes from the rat were collected and these leukocytes, that readily express TLR4-NF $\kappa$ B pathway factors, were stimulated *in vitro* as previously described (Noor et al. 2017; Sanchez et al. 2017). Because D2 receptors expressed on leukocytes are activated by pramipexole, and transcriptionally upregulate IL-10 (Besser, Ganor, and Levite 2005), dexpramipexole was examined in the current experiment to address the possibility that D2-independent actions can enhance IL-10 mRNA following immunological priming. Following deep isoflurane (10 min in 5% isoflurane and in oxygen at 2 L/min) anesthesia and rapid transcardial perfusion with ice cold 0.1 M phosphate buffered saline (PBS; pH = 7.4; flow rate 10 mL/min) the spleen was collected, and hand homogenized using a sterilized glass tissue homogenizer. Splenocytes were isolated and resuspended in RPMI 1640 complete medium supplemented with 10% (v/v) fetal bovine serum (FBS) (Sigma-Aldrich), 2.0 mM L-glutamine (Thermos Fisher Scientific, PA, USA), 50  $\mu$ M 2-mercaptoethanol (Sigma-Aldrich), 100 U/ml penicillin and 100  $\mu$ g/ml streptomycin (Thermos Fisher Scientific, PA, USA) to a cell density of 0.4 million cells/well in a 24-well culture plate (Corning Costar, Sigma-Aldrich). Each condition is conducted in triplicate. Resting cultured splenic leukocytes typically require immunological priming to observe cytokine production, including IL-10 (Kakugawa et al. 2000; Fiorentino et al. 1991). Cells were either unstimulated, or to induce immunological priming, stimulated with 1  $\mu$ g/ml lipopolysaccharide (LPS; diluted in RPMI; Sigma-Aldrich, St. Louis, MO, USA). Stimulated cells were treated with or without 2  $\mu$ g/ml dexpramipexole at 37 °C. As guidance, we followed a dose used in a human monocyte-derived osteoclast cell culture (0.5ug) study (Hanami et al. 2013), and included a 100-fold lower dose. Following a 24-h stimulation with LPS, cells were collected and stored in Qiazol Lysis Reagent (Qiazol; Qiagen; Cat#79306), at -80 °C for RNA extraction. Longer LPS duration incubation times under these conditions can generate spurious cellular responses unrelated to the treatment conditions.

## RNA extraction and quantitative real-time PCR for IL-10 detection

Total RNA was extracted as described previously (Noor et al. 2019; Vanderwall et al. 2017). Briefly, extraction was performed using the miRNeasy Micro Kit (Qiagen; Cat#217084) per manufacturer's instructions except where noted. Homogenization was performed using a motorized VWR disposable pellet mixer and cordless mortar pestle system (VWR; cordless pestle motor: Cat#47747-370; 1.5 mL microtubes: Cat#47747-362; 1.5 mL pestle: Cat#47747-358 followed by addition of Qiazol Lysis Reagent. See Noor et al., (Noor et al. 2019) for further details.

Once collected, total RNA samples were diluted to a standardized RNA concentration. Total RNA (0.9–1.2 µg) was used to synthesize cDNA. For reverse transcription (cDNA), SuperScript™ IV VIL0™ cDNA Synthesis Kit (Invitrogen) was used per manufacturer's instructions. The levels of mRNA transcripts were measured and analyzed, as previously described (Noor et al. 2019). The 1:200 dilutions of cDNA were used for assessment of the normalizer transcripts (18s RNA) for each of the tissue samples. Levels of IL-10 mRNA as well as 18s rRNA (*Rn18s*) were assayed in triplicate via quantitative real-time PCR (qRT-PCR) with Taqman Gene Expression Assays (cat# 4351370, ThermoFisher Scientific). In cases of triplicates with standard deviation of more than 0.1, the average value of the two closest replicates were included. All selected gene expression assays were identified by the manufacturer to be the “best coverage” assays, and designed to exclude detection of genomic DNA. Relative mRNA levels were analyzed with the formula:  $C = 2^{CTNormalizer} / 2^{CTTarget}$ , as previously described (Livak and Schmittgen 2001).

## Statistical analysis

Behavioral statistical analyses for i.v. pramipexole and dexpramipexole were performed using GraphPad Prism version 9.4.0. The assumption of sphericity was assessed using Mauchly's Test of Sphericity ( $\alpha = 0.05$ ) and if the assumption of sphericity was violated ( $p < 0.05$ ), the reported degrees of freedom and p-values were adjusted using the applicable Greenhouse-Geisser correction to protect against Type-I errors. Analyses of ipsilateral hindpaw behavioral thresholds were conducted separately from contralateral hindpaw thresholds. A one-way analysis of variance (ANOVA) was performed to assess differences in hindpaw sensitivity between groups at BL, and a two-way repeated measures ANOVA was conducted after sciatic nerve manipulation, at Days 3, 7 & 10 post-surgery. Additionally, to detect main effects of sciatic nerve manipulation and drug treatment, a two-way repeated measures ANOVA was conducted at 0 (day 10 prior to drug injection), 1, 2, 3, 24, 48 & 72 hrs (pramipexole) or at 0, 1, 2, 24 and 48 hrs (dexpramipexole) after injection. Tukey's multiple comparison's test was performed for all *post hoc* analyses at each timepoint to make comparisons between each treatment group. All hindpaw sensitivity data was graphed using GraphPad Prism version 9.4.0 (GraphPad Software Inc.; RRID:SCR\_002798) and presented as the mean  $\pm$  standard error of the mean (SEM). Analyses of IL-1 $\beta$  protein production from THP-1 cell culture was conducted applying a 2-way ANOVA. Analyses of IL-10 mRNA cytokine levels from rat splenocyte cell culture were performed applying a one-way ANOVA using GraphPad Prism version 9.4.0. All graphics data are represented as mean  $\pm$  standard error of the mean (SEM).

## Results.

### Pramipexole (Px) fully reverses CCI allodynia in mice.

At baseline (BL), mice displayed no significant differences in hindpaw sensitivity (ipsilateral:  $F_{3,20} = 1.628$ ,  $p = 0.215$ ; contralateral:  $F_{3,20} = 0.158$ ,  $p = 0.924$ ) (Fig. 1A & B), in support of our prior reports. Following surgical manipulation, CCI mice displayed an increase in hindpaw sensitivity during a 10-day timecourse (Fig. 1A & B), with a main effect of time (ipsilateral:  $F_{1.7,34.6} = 27.91$ ,  $p < 0.0001$ ; contralateral:  $F_{1.8,35.3} = 27.75$ ,  $p < 0.0001$ ), surgery (ipsilateral:  $F_{3,20} = 139.8$ ,  $p < 0.0001$ ; contralateral:  $F_{3,20} = 134.4$ ,  $p < 0.0001$ ), and an interaction between time and surgery (ipsilateral:  $F_{6,40} = 9.29$ ,  $p < 0.0001$ ; contralateral:  $F_{6,40} = 10.63$ ,  $p < 0.0001$ ). Sham-operated mice revealed hindpaw responses similar to BL levels throughout the timecourse. Following hindpaw assessment, mice received i.v. Px on Day 10 and revealed a complete reversal from allodynia within 1 hr that persisted through 3 hrs, with allodynia returning by 24 hrs and remaining stable through 72 hrs, as demonstrated by a main effect of CCI surgery (ipsilateral:  $F_{1,70} = 1059$ ,  $p < 0.0001$ ; contralateral:  $F_{1,70} = 893.8$ ,  $p < 0.0001$ ), Px treatment (ipsilateral:  $F_{1,70} = 135.4$ ,  $p < 0.0001$ ; contralateral:  $F_{1,70} = 113.0$ ,  $p < 0.0001$ ), and interactions between CCI surgery and Px treatment (ipsilateral:  $F_{1,70} = 92.34$ ,  $p < 0.0001$ ; contralateral:  $F_{1,70} = 102.7$ ,  $p < 0.0001$ ), and time (ipsilateral:  $F_{6,70} = 26.89$ ,  $p < 0.0001$ ; contralateral:  $F_{6,70} = 16.94$ ,  $p < 0.0001$ ), was observed (Fig. 1A & B).

### Dexpramipexole (DPX) fully reverses CCI allodynia in mice.

At baseline (BL), mice did not display significant differences in hindpaw sensitivity (ipsilateral:  $F_{3,16} = 0.561$ ,  $p = 0.6486$ ; contralateral:  $F_{3,16} = 0.1454$ ,  $p = 0.9312$ ) (Fig. 2A & B). However, following CCI manipulation, mice displayed an increase in hindpaw sensitivity over a 10-day timecourse relative BL thresholds (Fig 2A & B), with a main effect of time (ipsilateral:  $F_{2.3,30.0} = 28.47$ ,  $p < 0.0001$ ; contralateral:  $F_{2.6,42.2} = 8.73$ ,  $p < 0.001$ ), surgery (ipsilateral:  $F_{1,16} = 68.12$ ,  $p < 0.0001$ ; contralateral:  $F_{1,16} = 28.16$ ,  $p < 0.001$ ), and an interaction between time and surgery (ipsilateral:  $F_{3,48} = 17.70$ ,  $p < 0.0001$ ; contralateral:  $F_{3,48} = 11.00$ ,  $p < 0.0001$ ). Sham-operated mice revealed hindpaw responses similar to BL levels throughout the timecourse.

By Day 10, CCI-treated mice were fully allodynic bilaterally relative to sham treated mice (Fig. 2A & B) (ipsilateral:  $F_{3,16} = 55.06$ ,  $p < 0.0001$ ; contralateral:  $F_{3,16} = 11$ ,  $p < 0.0005$ ). Following hindpaw assessment, mice received i.v. DPX (0.5  $\mu\text{g}$ ), a dose that revealed efficacy from Px treatment. Thus, analyses supported a main effect of sciatic nerve manipulation (Sham vs. CCI) on hindpaw thresholds (ipsilateral:  $F_{0.68,5.4} = 704.2$ ,  $p < 0.0001$ ; contralateral:  $F_{0.51,4.9} = 688.7$ ,  $p < 0.0001$ ), a main effect of DPX treatment (ipsilateral:  $F_{1,8} = 43.77$ ,  $p < 0.0005$ ; contralateral:  $F_{1,8} = 20.37$ ,  $p < 0.005$ ), an interaction between time and DPX treatment (ipsilateral:  $F_{3,24} = 22.22$ ,  $p < 0.0001$ ; contralateral:  $F_{3,24} = 6.07$ ,  $p < 0.005$ ), and an interaction of CCI, DPX treatment and time (ipsilateral:  $F_{2,24} = 7.946$ ,  $p < 0.001$ ; contralateral:  $F_{2,24} = 7.33$ ,  $p < 0.005$ ) impacting hindpaw thresholds. Notably, compared to vehicle-treated allodynic mice, a complete reversal from allodynia was observed within 1 hr that persisted through 2 hrs, with allodynia returning by 24 hrs and remaining stable at the last time point assessed, 48 hrs ( $p < 0.0001$ ).

### **Pramipexole (Px) treatment suppresses IL-1 $\beta$ release in activated human monocytes.**

Pramipexole suppresses the pro-nociceptive cytokine, interleukin-1beta (IL-1 $\beta$ ) from being released from human monocytes after classic TLR-4 immune cell stimulation with LPS (Fig. 3A). While Px (5 pg and 500 pg) does not significantly alter basal cellular levels of IL-1 $\beta$  protein, LPS in the absence of Px significantly elevates IL-1 $\beta$  protein ( $F_{1,17} = 40.56$ ,  $p < 0.001$ ). However, both 5 pg and 500 pg of Px in the presence of LPS stimulation significantly blunts IL-1 $\beta$  release ( $F_{2,17} = 5.158$ ,  $p < 0.02$ ). These doses given to isolated human monocyte cells in culture are 10,000 and 1000-fold lower than doses given to mice for *in vivo* application to reverse allodynia (Fig. 1A & B).

### **Dexpramipexole (DPX) treatment increases IL-10 production in TLR4-activated splenocytes.**

Providing evidence for direct anti-inflammatory actions of DPX, splenocytes produce enhanced anti-inflammatory IL-10 cytokine levels in the presence of DPX (Fig. 3B). Compared to untreated isolated splenocytes, LPS induces a predictable and robust increase in IL-10 mRNA levels, with DPX inducing further IL-10 mRNA production despite the continuous challenge of LPS. A one-way ANOVA revealed DPX generated a significant increase in IL-10 mRNA ( $F_{2,6} = 16.37$ ,  $p < 0.005$ ). The additional elevation of IL-10 production in response to DPX with LPS is a compensatory endogenous response to mitigate the impact of powerful proinflammatory actions stimulated from the activation of the TLR-4 receptor.

## **Discussion**

The current report demonstrates that FDA-approved pramipexole ((-)-pramipexole), a D2/D3-preferring agonist, transiently reverses chronic bilateral allodynia induced by sciatic nerve damage using the well-characterized CCI model (Bennett and Xie 1988) (Fig. 1). The observed bilateral allodynia is supported by previous reports utilizing the CCI model in the rat and the mouse (Noor et al. 2020; Noor S 2018; Wilkerson et al. 2020; Wilkerson et al. 2022; Dubovy et al. 2007; Hatashita et al. 2008; Kleinschnitz et al. 2005; Ruohonen et al. 2002; Schreiber, Beitz, and Wilcox 2008). Additionally, these published reports show concurrent spinal cord NF- $\kappa$ B and cytokine alterations and bilateral glial activation following CCI (Noor et al. 2019; Vanderwall et al. 2017; Wilkerson et al. 2020; Wilkerson et al. 2022). NF- $\kappa$ B is a transcription factor important in the production of proinflammatory cytokines including IL-1 $\beta$  (Niederberger and Geisslinger 2008; Molina-Holgado et al. 2003; Ozaktay et al. 2006; Samad et al. 2004; Viviani et al. 2003; Wieseler-Frank et al. 2004), and other rodent models of pathological pain have demonstrated involvement of the TLR4-NF $\kappa$ B-inflammatory cytokine cascade (Grace et al. 2021; Woller et al. 2016). The neuroimmune contribution to pathological pain is speculated to occur when damaged axons of nociceptors release several endogenous cell-stress signaling molecules within the dorsal horn of the spinal cord and activate locally expressed TLR4 innate immune receptors expressed mostly on surrounding glial cells (astrocytes and microglia). TLR4-induced glial activation results in proinflammatory cytokine release, including IL-1 $\beta$ , acting on post-synaptic neurons as well as perisynaptic glia. Thus, the TLR4-mediated neuroimmune process has been characterized to play a key role in pathological pain induced in a wide

range of animal models (Grace et al. 2018; Hutchinson et al. 2008; Watkins et al. 2009). Together, these prior reports and the current data strongly suggest that the anti-allodynic effects of both pramipexole and dexpramipexole examined in the chronic CCI model may likely extend to a variety of these other widely-used neuropathic pain models.

The anti-inflammatory actions of pramipexole were demonstrated in mouse models of hindpaw inflammation (e.g., carrageenan, formalin or 12-O-tetradecanoylphorbol-13-acetate (TPA), whereby, a substantial reduction in local neutrophil infiltration and subcutaneous edema following pramipexole treatment was observed. These observations established that pramipexole acted independently of antioxidant mechanisms in the anti-inflammatory response (Sadeghi et al. 2017). The pain-suppressive effects of pramipexole acting via anti-inflammatory mechanisms was demonstrated when pramipexole reduced spinal levels of NF- $\kappa$ B and IL-1 $\beta$  in rats with mechanical allodynia caused by subcutaneous formalin in the dorsal surface of the hind paw, an established model of inflammatory pain (Santamaria-Anzures et al. 2023).

However, it is not well-understood how pramipexole may act to reduce NF- $\kappa$ B activation and subsequent and IL-1 $\beta$ . One possibility may through pramipexole's action on D2. Indeed, D2 is expressed on pathologically activated resident microglia, and on peripherally derived macrophages, (Huck et al. 2015), as well as on astrocytes, with D2 generally characterized to couple to inhibitory G $\alpha$ i protein (Rangel-Barajas, Coronel, and Floran 2015; Sibley, Monsma, and Shen 1993). Upon D2-specific agonist activation, stimulated astrocytes reduce IL-1 $\beta$  production (Zhu et al. 2018). Thus, while speculative, it is possible that pramipexole may act to reduce TLR4-mediated spinal glial activation and consequent NF- $\kappa$ B-IL-1 $\beta$  induction through activation of spinal D2. In support of pramipexole's anti-inflammatory actions, data from the current studies using THP-1 immune-stimulated cultured cells that express high levels of TLR4 revealed suppressed IL-1 $\beta$  protein levels when treated with pramipexole (Fig. 3A). Notably, immune cells like THP-1 cells express D2 receptors suggesting the possible involvement of D2 actions. It is important to point out that receptors for dopamine (D2/D3) are distributed throughout the spinal cord dorsoventral axis (Zhu et al. 2007), and dopamine plays key regulatory roles in spinal cord pain modulation through inhibition of nociceptive relays at the level of the dorsal horn spinal cord (Garcia-Ramirez et al. 2014; Tamae et al. 2005). It is an intriguing possibility that pramipexole impacts the neuroimmune-D2 interface to treat in chronic pain; however, more work is needed to explore this possibility.

While pramipexole may be a promising therapeutic for off-label application of treating pathological pain, a drawback is the widespread D2/D3 expression throughout the CNS resulting in non-specific side-effects. The current report utilized the clinically-approved dexpramipexole ((+)-pramipexole)) to analyze its anti-allodynic effects with minimal D2/D3 action. The data show a similar pattern of transient anti-allodynia by dexpramipexole that is similar to that observed with pramipexole. That is, dexpramipexole transiently reversed CCI-induced bilateral allodynia within 1 hr of administration with allodynia returning by 24 hours and remaining stably allodynic thereafter (Fig. 2). These data support the prior work showing the anti-allodynic actions of CCI-nerve damage (Urru et al. 2020). In work by Urru and colleagues, dexpramipexole binds the specific voltage-gated sodium

channel (Nav) 1.8, (Urru et al. 2020), which is present within peripheral and spinal central terminals of primary nociceptors (Waxman and Zamponi 2014). Peripheral administration of dexpramipexole demonstrates activity as a neuronal Nav1.8 antagonist and acutely reduces the nociceptive behavior induced by inflammatory pain from hindpaw formalin injection or induction of ankle arthritis, or in the mouse neuropathic pain models such as sciatic nerve damage, chemotherapy- and diabetic-induced neuropathy (Urru et al. 2020). The current report administered dexpramipexole peripherally, and therefore, it is entirely possible that the anti-allodynic effects of dexpramipexole are via its action at Nav1.8. However, it is additionally possible that the actions of dexpramipexole as a potential pain therapeutic may also involve reduced levels of IL-1 $\beta$  at the level of the spinal cord.

The current report adds to prior reports demonstrating the observed bilateral of allodynia induced by unilateral CCI, which reflects pathological nociceptive signaling at the level of the spinal cord (Noor et al. 2020; Noor S 2018; Wilkerson et al. 2020; Wilkerson et al. 2022; Dubovy et al. 2007; Hatashita et al. 2008; Kleinschnitz et al. 2005; Ruohonen et al. 2002; Schreiber, Beitz, and Wilcox 2008). Spinal cords of animals with bilateral allodynia were characterized with bilateral glial activation and a variety of proinflammatory factors (Noor et al. 2019; Vanderwall et al. 2017; Wilkerson et al. 2020; Wilkerson et al. 2022). The observed bilateral allodynia in mice from the current report and bilateral reversal from allodynia from i.v. pramipexole and, separately, dexpramipexole, suggests that their anti-allodynic actions occur not only at Nav1.8 channels on nociceptive fibers, but also at the level of the spinal cord. The current report utilized rat splenocytes to complement Urru and colleagues (Urru et al. 2020) who demonstrated that dexpramipexole impacts sodium currents in rat sensory ganglion cells. Results from the cultured splenocytes treated with dexpramipexole revealed significantly elevated mRNA expression levels of the potent anti-inflammatory cytokine IL-10 (Fig. 3B). However, these data do not test the possibility that dexpramipexole may induce IL-10 production without requiring splenocyte stimulation; that dexpramipexole may raise basal levels of IL-10 production. Despite this drawback, these results are complementary to existing reports, as a number of studies have examined the impact of dexpramipexole on rat neurons (Alavian et al. 2012; Cao et al. 2016; Coppi et al. 2021; Coppi et al. 2018; Gribkoff and Bozik 2008; Urru et al. 2020), and rat immune cells utilized in the current report provides additional information on the neuroimmune-specific actions of dexpramipexole. Given that dexpramipexole has significantly reduced D2/D3 activity (Gribkoff and Bozik 2008), the anti-inflammatory actions of dexpramipexole likely occur through D2/D3-independent mechanisms, which is worthy of further investigation. While dexpramipexole is a promising pain therapeutic, additional studies are needed to examine its IL-10 enhancing effects in peripheral neuroimmune and CNS neuroimmune actions.

Due to the anti-inflammatory properties of dexpramipexole, its application may extend beyond solely treating neuropathic pain. Indeed, high comorbidity rates for chronic pain, sleep disorders, and depression exists, and treating pain may also benefit the treatment for depression (Cohen and Mao 2014). For example, patients with neuropathic pain caused by nerve injury usually present with co-morbid affective changes including depression. Reports show that neuroglia may play a role in the development of depression, just as they do in the development of neuropathic pain. As such, it has been suggested that

neuroglia in neuropathic pain also play a key role with the development of depression in pain patients (Liu et al. 2021). There is a strong link between brain glial inflammatory cytokines and depression (Jeon and Kim 2017), thus, implicating the local actions of proinflammatory cytokines and the possible benefit of elevated expression of the endogenous anti-inflammatory cytokine, IL-10. While pramipexole has been reported to induce promising responses in chronic and severe treatment-resistant depressed patients, including bipolar disorder (Fawcett et al. 2016), and the potential anti-inflammatory actions of pramipexole have been hypothesized to facilitate the anti-depressive efficacy in preclinical models (Lieberknecht et al. 2017) and clinically (Escalona and Fawcett 2017), it is possible that dexpramipexole may be a better target and could provide a blueprint for future therapeutics aimed at controlling neuropathic pain and depression co-morbidities without the possible unintended side effects of acting at D2/D3 throughout the brain.

In summary, the data reported herein confirm and extend prior reports that FDA-approved ((-)-pramipexole), and its enantiomer, dexpramipexole ((+)-pramipexole) that is clinically approved, both with good safety profiles, are therapeutically viable agents for treating chronic neuropathic pain, and may provide a blueprint for next-generation pain therapeutics. While more work is needed to better understand the pleiotropic mechanisms of pramipexole and dexpramipexole, the low doses utilized in the current report that produced robust anti-allodynia support their therapeutic promise as compounds capable of pain control without creating analgesia. Moreover, multifaceted approaches for pain treatment have been emerging, and pramipexole and dexpramipexole may fulfill the necessity to target more than one underlying mechanism in the etiological development of pathological pain such as targeting D2/D3 actions, anti-inflammatory pathways, and/or inhibiting Nav1.8 signaling.

## Acknowledgments

We are greatly appreciative to the New Mexico Alcohol Research Center for their continuous support in providing intellectual and collaborative supportive of these studies.

## Funding

This study was funded by the National Institutes of Alcoholism and Alcohol Abuse (NIAAA) (R21-AA023051), (R01-AA025967), (T32-AA014127), (P50-AA022534), and NIH/NCATS (5UL1TR001449)

## Data Availability Statement

The datasets presented in this study will be found in the online repositories, Mendeley

## Bibliography

- Alavian KN, Dworetzky SI, Bonanni L, Zhang P, Sacchetti S, Mariggio MA, Onofrj M, Thomas A, Li H, Mangold JE, Signore AP, Demarco U, Demady DR, Nabili P, Lazrove E, Smith PJ, Gribkoff VK, and Jonas EA. 2012. 'Effects of dexpramipexole on brain mitochondrial conductances and cellular bioenergetic efficiency', *Brain research*, 1446: 1–11. [PubMed: 22364637]
- Andersson U, Tracey KJ, and Yang H. 2021. 'Post-Translational Modification of HMGB1 Disulfide Bonds in Stimulating and Inhibiting Inflammation', *Cells*, 10.
- Aurell CA, Hawley ME, and Wistrom AO. 1999. 'Direct visualization of gram-negative bacterial lipopolysaccharide self-assembly', *Mol Cell Biol Res Commun*, 2: 42–6. [PubMed: 10527890]

- Bennett GJ, and Xie KY. 1988. 'A peripheral mononeuropathy in rat that produces disorders of pain sensation like those seen in man', *Pain*, 33: 87–107. [PubMed: 2837713]
- Besser MJ, Ganor Y, and Levite M. 2005. 'Dopamine by itself activates either D2, D3 or D1/D5 dopaminergic receptors in normal human T-cells and triggers the selective secretion of either I-L-10, TNFalpha or both', *J Neuroimmunol*, 169: 161–71. [PubMed: 16150496]
- Bonin RP, Bories C, and De Koninck Y. 2014. 'A simplified up-down method (SUDO) for measuring mechanical nociception in rodents using von Frey filaments', *Mol Pain*, 10: 26. [PubMed: 24739328]
- Bottero V, Imbert V, Frelin C, Formento JL, and Peyron JF. 2003. 'Monitoring NF-kappa B transactivation potential via real-time PCR quantification of I kappa B-alpha gene expression', *Mol Diagn*, 7: 187–94. [PubMed: 15068390]
- Cao LF, Peng XY, Huang Y, Wang B, Zhou FM, Cheng RX, Chen LH, Luo WF, and Liu T. 2016. 'Restoring Spinal Noradrenergic Inhibitory Tone Attenuates Pain Hypersensitivity in a Rat Model of Parkinson's Disease', *Neural Plast*, 2016: 6383240. [PubMed: 27747105]
- Carville SF, Arendt-Nielsen L, Bliddal H, Blotman F, Branco JC, Buskila D, Da Silva JA, Danneskiold-Samsøe B, Dincer F, Henriksson C, Henriksson KG, Kosek E, Longley K, McCarthy GM, Perrot S, Puszczewicz M, Sarzi-Puttini P, Silman A, Spath M, Choy EH, and Eular. 2008. 'EULAR evidence-based recommendations for the management of fibromyalgia syndrome', *Ann Rheum Dis*, 67: 536–41. [PubMed: 17644548]
- Chaplan SR, Bach FW, Pogrel JW, Chung JM, and Yaksh TL. 1994. 'Quantitative assessment of tactile allodynia in the rat paw', *J. Neurosci. Meth*, 53: 55–63.
- Cohen SP, and Mao J. 2014. 'Neuropathic pain: mechanisms and their clinical implications', *BMJ*, 348: f7656. [PubMed: 24500412]
- Cohen SP, Vase L, and Hooten WM. 2021. 'Chronic pain: an update on burden, best practices, and new advances', *Lancet*, 397: 2082–97. [PubMed: 34062143]
- Coppi E, Buonvicino D, Ranieri G, Cherchi F, Venturini M, Pugliese AM, and Chiarugi A. 2021. 'Dexramipexole Enhances K(+) Currents and Inhibits Cell Excitability in the Rat Hippocampus In Vitro', *Mol Neurobiol*, 58: 2955–62. [PubMed: 33566318]
- Coppi E, Lana D, Cherchi F, Fusco I, Buonvicino D, Urru M, Ranieri G, Muzzi M, Iovino L, Giovannini MG, Pugliese AM, and Chiarugi A. 2018. 'Dexramipexole enhances hippocampal synaptic plasticity and memory in the rat', *Neuropharmacology*, 143: 306–16. [PubMed: 30291939]
- Cudkowicz M, Bozik ME, Ingersoll EW, Miller R, Mitsumoto H, Shefner J, Moore DH, Schoenfeld D, Mather JL, Archibald D, Sullivan M, Amburgey C, Moritz J, and Gribkoff VK. 2011. 'The effects of dexramipexole (KNS-760704) in individuals with amyotrophic lateral sclerosis', *Nat Med*, 17: 1652–6. [PubMed: 22101764]
- Cudkowicz ME, van den Berg LH, Shefner JM, Mitsumoto H, Mora JS, Ludolph A, Hardiman O, Bozik ME, Ingersoll EW, Archibald D, Meyers AL, Dong Y, Farwell WR, Kerr DA, and Empower investigators. 2013. 'Dexramipexole versus placebo for patients with amyotrophic lateral sclerosis (EMPOWER): a randomised, double-blind, phase 3 trial', *Lancet Neurol*, 12: 1059–67. [PubMed: 24067398]
- Donnelly CR, Chen O, and Ji RR. 2020. 'How Do Sensory Neurons Sense Danger Signals?', *Trends in neurosciences*, 43: 822–38. [PubMed: 32839001]
- Donnelly RP, Dickensheets H, and Finbloom DS. 1999. 'The interleukin-10 signal transduction pathway and regulation of gene expression in mononuclear phagocytes', *J. Interferon Cytokine Res*, 19: 563–73. [PubMed: 10433356]
- Dowdall T, Robinson I, and Meert TF. 2005. 'Comparison of five different rat models of peripheral nerve injury', *Pharmacology, biochemistry, and behavior*, 80: 93–108. [PubMed: 15652385]
- Dubovy P, Tuckova L, Jancalek R, Svizenska I, and Klusakova I. 2007. 'Increased invasion of ED-1 positive macrophages in both ipsi- and contralateral dorsal root ganglia following unilateral nerve injuries', *Neurosci Lett*, 427: 88–93. [PubMed: 17931774]
- Eidinoff A, Sathivadivel N, McBride T, Parker A, Okeagu C, Kaye AD, Kaye AM, Kaye JS, Kaye RJ, Sheth M M, Viswanath O, and Urits I. 2020. 'Chronic Pain Treatment Strategies in Parkinson's Disease', *Neurol Int*, 12: 61–76. [PubMed: 33218135]



- Edwards BS, Young SM, Oprea TI, Bologna CG, Prossnitz ER, and Sklar LA. 2006. 'Biomolecular screening of formylpeptide receptor ligands with a sensitive, quantitative, high-throughput flow cytometry platform', *Nat Protoc*, 1: 59–66. [PubMed: 17406212]
- Edwards S, Callicoatte CN, Barattini AE, Cucinello-Ragland JA, Melain A, Edwards KN, Gilpin NW, Avegno EM, and Pahng AR. 2022. 'Pramipexole treatment attenuates mechanical hypersensitivity in male rats experiencing chronic inflammatory pain', *Neuropharmacology*, 208: 108976. [PubMed: 35085583]
- Escalona R, and Fawcett J. 2017. 'Pramipexole in Treatment Resistant-Depression, Possible Role of Inflammatory Cytokines', *Neuropsychopharmacology*, 42: 363. [PubMed: 27909317]
- Fawcett J, Rush AJ, Vukelich J, Diaz SH, Dunklee L, Romo P, Yarns BC, and Escalona R. 2016. 'Clinical Experience With High-Dosage Pramipexole in Patients With Treatment-Resistant Depressive Episodes in Unipolar and Bipolar Depression', *Am J Psychiatry*, 173: 107–11. [PubMed: 26844792]
- Fawzy HA, Mohammed AA, Fawzy HM, and Fikry EM. 2022. 'Reorienting of pramipexole as a promising therapy for acute pancreatitis in a rat model by suppressing TLR4/NF-kappaB p65/NLRP3 inflammasome signaling', *Can J Physiol Pharmacol*, 100: 542–52. [PubMed: 35413206]
- Fiorentino DF, Zlotnik A, Vieira P, Mosmann TR, Howard M, Moore KW, and O'Garra A. 1991. 'IL-10 acts on the antigen-presenting cell to inhibit cytokine production by Th1 cells', *J Immunol*, 146: 3444–51. [PubMed: 1827484]
- Garcia-Ramirez DL, Calvo JR, Hochman S, and Quevedo JN. 2014. 'Serotonin, dopamine and noradrenaline adjust actions of myelinated afferents via modulation of presynaptic inhibition in the mouse spinal cord', *PLoS One*, 9: e89999. [PubMed: 24587177]
- Ghosh TK, Mickelson DJ, Fink J, Solberg JC, Inglefield JR, Hook D, Gupta SK, Gibson S, and Alkan SS. 2006. 'Toll-like receptor (TLR) 2–9 agonists-induced cytokines and chemokines: I. Comparison with T cell receptor-induced responses', *Cell Immunol*, 243: 48–57. [PubMed: 17250816]
- Gonzalez P, Burgaya F, Acarin L, Peluffo H, Castellano B, and Gonzalez B. 2009. 'Interleukin-10 and interleukin-10 receptor-I are upregulated in glial cells after an excitotoxic injury to the postnatal rat brain', *Journal of neuropathology and experimental neurology*, 68: 391–403. [PubMed: 19287312]
- Gossard TR, Trotti LM, Videnovic A, and St Louis EK. 2021. 'Restless Legs Syndrome: Contemporary Diagnosis and Treatment', *Neurotherapeutics*, 18: 140–55. [PubMed: 33880737]
- Grace PM, Strand KA, Galer EL, Rice KC, Maier SF, and Watkins LR. 2018. 'Protraction of neuropathic pain by morphine is mediated by spinal damage associated molecular patterns (DAMPs) in male rats', *Brain, behavior, and immunity*, 72: 45–50. [PubMed: 28860068]
- Grace PM, Tawfik VL, Svensson CI, Burton MD, Loggia ML, and Hutchinson MR. 2021. 'The Neuroimmunology of Chronic Pain: From Rodents to Humans', *J Neurosci*, 41: 855–65. [PubMed: 33239404]
- Greenhill CJ, Jones GW, Nowell MA, Newton Z, Harvey AK, Moideen AN, Collins FL, Bloom AC, Coll RC, Robertson AA, Cooper MA, Rosas M, Taylor PR, O'Neill LA, Humphreys IR, Williams AS, and Jones SA. 2014. 'Interleukin-10 regulates the inflammasome-driven augmentation of inflammatory arthritis and joint destruction', *Arthritis Res Ther*, 16: 419. [PubMed: 25175678]
- Gribkoff VK, and Bozik ME. 2008. 'KNS-760704 [(6R)-4,5,6,7-tetrahydro-N6-propyl-2, 6-benzothiazole-diamine dihydrochloride monohydrate] for the treatment of amyotrophic lateral sclerosis', *CNS Neurosci Ther*, 14: 215–26. [PubMed: 18801114]
- Hanami K, Nakano K, Saito K, Okada Y, Yamaoka K, Kubo S, Kondo M, and Tanaka Y. 2013. 'Dopamine D2-like receptor signaling suppresses human osteoclastogenesis', *Bone*, 56: 1–8. [PubMed: 23631878]
- Hatashita S, Sekiguchi M, Kobayashi H, Konno S, and Kikuchi S. 2008. 'Contralateral neuropathic pain and neuropathology in dorsal root ganglion and spinal cord following hemilateral nerve injury in rats', *Spine*, 33: 1344–51. [PubMed: 18496347]
- Hauser RA, Schapira AH, Barone P, Mizuno Y, Rascol O, Busse M, Debieuvre C, Fraessdorf M, Poewe W, and Studies Group Pramipexole ER. 2014. 'Long-term safety and sustained efficacy

- of extended-release pramipexole in early and advanced Parkinson's disease', *Eur J Neurol*, 21: 736–43. [PubMed: 24834511]
- He Y, Franchi L, and Nunez G. 2013. 'TLR agonists stimulate Nlrp3-dependent IL-1beta production independently of the purinergic P2X7 receptor in dendritic cells and in vivo', *J Immunol*, 190: 334–9. [PubMed: 23225887]
- Hitchins VM, and Merritt K. 1999. 'Decontaminating particles exposed to bacterial endotoxin (LPS)', *J Biomed Mater Res*, 46: 434–7. [PubMed: 10398002]
- Huck JH, Freyer D, Bottcher C, Mladinov M, Muselmann-Genschow C, Thielke M, Gladow N, Bloomquist D, Mergenthaler P, and Priller J. 2015. 'De novo expression of dopamine D2 receptors on microglia after stroke', *J Cereb Blood Flow Metab*, 35: 1804–11. [PubMed: 26104289]
- Hutchinson MR, Zhang Y, Brown K, Coats BD, Shridhar M, Sholar PW, Patel SJ, Crysdale NY, Harrison JA, Maier SF, Rice KC, and Watkins LR. 2008. 'Non-stereoselective reversal of neuropathic pain by naloxone and naltrexone: involvement of toll-like receptor 4 (TLR4)', *Eur J Neurosci*, 28: 20–9. [PubMed: 18662331]
- Jakopin Z, and Corsini E. 2019. 'THP-1 Cells and Pro-inflammatory Cytokine Production: An in Vitro Tool for Functional Characterization of NOD1/NOD2 Antagonists', *Int J Mol Sci*, 20.
- Jeon SW, and Kim YK. 2017. 'Inflammation-induced depression: Its pathophysiology and therapeutic implications', *J Neuroimmunol*, 313: 92–98. [PubMed: 29153615]
- Kakugawa K, Uda K, Nakashima K, Inaba K, Oka Y, Sugiyama H, Tamamura H, and Yamagishi H. 2000. 'Efficient induction of peptide-specific cytotoxic T lymphocytes by LPS-activated spleen cells', *Microbiol Immunol*, 44: 123–33. [PubMed: 10803499]
- Kato J, Agalave NM, and Svensson CI. 2016. 'Pattern recognition receptors in chronic pain: Mechanisms and therapeutic implications', *Eur J Pharmacol*, 788: 261–73. [PubMed: 27343378]
- Kleinschnitz C, Brinkhoff J, Sommer C, and Stoll G. 2005. 'Contralateral cytokine gene induction after peripheral nerve lesions: dependence on the mode of injury and NMDA receptor signaling', *Brain research. Molecular brain research*, 136: 23–8. [PubMed: 15893583]
- Lee SI, Hoeijmakers JGJ, Faber CG, Merckies ISJ, Lauria G, and Waxman SG. 2020. 'The small fiber neuropathy NaV1.7 I228M mutation: impaired neurite integrity via bioenergetic and mitotoxic mechanisms, and protection by dextramipexole', *J Neurophysiol*, 123: 645–57. [PubMed: 31851560]
- Lieberknecht V, Cunha MP, Junqueira SC, Coelho ID, de Souza LF, Dos Santos AR, Rodrigues AL, Dutra RC, and Dafre AL. 2017. 'Antidepressant-like effect of pramipexole in an inflammatory model of depression', *Behav Brain Res*, 320: 365–73. [PubMed: 27825895]
- Lin HY, Chang YY, Kao MC, and Huang CJ. 2017. 'Naloxone inhibits nod-like receptor protein 3 inflammasome', *J Surg Res*, 219: 72–77. [PubMed: 29078913]
- Liu GJ, Wu L, Lin Wang S, Xu LL, Ying Chang L, and Fu Wang Y. 2016. 'Efficacy of Pramipexole for the Treatment of Primary Restless Leg Syndrome: A Systematic Review and Meta-analysis of Randomized Clinical Trials', *Clin Ther*, 38: 162–79 e6. [PubMed: 26572941]
- Liu L, Yin Y, Li F, Malhotra C, and Cheng J. 2017. 'Flow cytometry analysis of inflammatory cells isolated from the sciatic nerve and DRG after chronic constriction injury in mice', *J Neurosci Methods*, 284: 47–56. [PubMed: 28445708]
- Liu Q, Li R, Yang W, Cui R, and Li B. 2021. 'Role of neuroglia in neuropathic pain and depression', *Pharmacol Res*, 174: 105957. [PubMed: 34688904]
- Livak KJ, and Schmittgen TD. 2001. 'Analysis of relative gene expression data using real-time quantitative PCR and the 2(-Delta Delta C(T)) Method', *Methods*, 25: 402–8. [PubMed: 11846609]
- Marcus DA. 2009. 'Fibromyalgia: diagnosis and treatment options', *Gend Med*, 6 Suppl 2: 139–51. [PubMed: 19406366]
- Martins CP, Paes RS, Baldasso GM, Ferrarini EG, Scussel R, Zaccaron RP, Machado-de-Avila RA, Lock Silveira PC, and Dutra RC. 2022. 'Pramipexole, a dopamine D3/D2 receptor-preferring agonist, attenuates reserpine-induced fibromyalgia-like model in mice', *Neural Regen Res*, 17: 450–58. [PubMed: 34269222]
- Martucci C, Trovato AE, Costa B, Borsani E, Franchi S, Magnaghi V, Panerai AE, Rodella LF, Valsecchi AE, Sacerdote P, and Colleoni M. 2008. 'The purinergic antagonist PPADS reduces pain

related behaviours and interleukin-1 beta, interleukin-6, iNOS and nNOS overproduction in central and peripheral nervous system after peripheral neuropathy in mice', *Pain*, 137: 81–95. [PubMed: 17900807]

- Mierau J, Schneider FJ, Ensinger HA, Chio CL, Lajiness ME, and Huff RM. 1995. 'Pramipexole binding and activation of cloned and expressed dopamine D2, D3 and D4 receptors', *Eur J Pharmacol*, 290: 29–36. [PubMed: 7664822]
- Milligan ED, Langer SJ, Sloane EM, He L, Wieseler-Frank J, O'Connor K, Martin D, Forsayeth JR, Maier SF, Johnson K, Chavez RA, Leinwand LA, and Watkins LR. 2005. 'Controlling pathological pain by adenovirally driven spinal production of the anti-inflammatory cytokine, interleukin-10', *Eur J Neurosci*, 21: 2136–48. [PubMed: 15869510]
- Milligan ED, Mehmert KK, Hinde JL, Harvey LO, Martin D, Tracey KJ, Maier SF, and Watkins LR. 2000. 'Thermal hyperalgesia and mechanical allodynia produced by intrathecal administration of the human immunodeficiency virus-1 (HIV-1) envelope glycoprotein, gp120', *Brain research*, 861: 105–16. [PubMed: 10751570]
- Milligan ED, Penzkover KR, Soderquist RG, and Mahoney MJ. 2012. 'Spinal interleukin-10 therapy to treat peripheral neuropathic pain', *Neuromodulation : journal of the International Neuromodulation Society*, 15: 520–6; discussion 26. [PubMed: 22672183]
- Milligan ED, Soderquist RG, Malone SM, Mahoney JH, Hughes TS, Langer SJ, Sloane EM, Maier SF, Leinwand LA, Watkins LR, and Mahoney MJ. 2006. 'Intrathecal polymer-based interleukin-10 gene delivery for neuropathic pain', *Neuron glia biology*, 2: 293–308. [PubMed: 18079973]
- Molina-Holgado F, Pinteaux E, Moore JD, Molina-Holgado E, Guaza C, Gibson RM, and Rothwell NJ. 2003. 'Endogenous interleukin-1 receptor antagonist mediates anti-inflammatory and neuroprotective actions of cannabinoids in neurons and glia', *J Neurosci*, 23: 6470–4. [PubMed: 12878687]
- Moore KW, de Waal Malefyt R, Coffman RL, and O'Garra A. 2001. 'Interleukin-10 and the interleukin-10 receptor', *Annu Rev Immunol*, 19: 683–765. [PubMed: 11244051]
- Niederberger E, and Geisslinger G. 2008. 'The IKK-NF-kappaB pathway: a source for novel molecular drug targets in pain therapy?', *FASEB J*, 22: 3432–42. [PubMed: 18559989]
- Noor S, Sanchez JJ, Pervin Z, Sanchez JE, M. Sun MS, Epler LT, Davies S, Savage DD, Mellios N, Jantzie LL, Milligan ED. 2018. 'Neuropathic pain susceptibility in prenatal alcohol exposed (PAE) females is mediated by the proinflammatory actions of lymphocyte function-associated antigen (LFA)-1 on immune and glial cells', *Neuroscience Meeting Planner*, San Diego, CA: Society for Neuroscience, 2018., *Peripheral Mechanisms of Neuropathic Pain*
- Noor S, Sanchez JJ, Sun MS, Pervin Z, Sanchez JE, Havard MA, Epler LT, Nysus MV, Norenberg JP, Wagner CR, Davies S, Wagner JL, Savage DD, Jantzie LL, Mellios N, and Milligan ED. 2020. 'The LFA-1 antagonist BIRT377 reverses neuropathic pain in prenatal alcohol-exposed female rats via actions on peripheral and central neuroimmune function in discrete pain-relevant tissue regions', *Brain, behavior, and immunity*, 87: 339–58. [PubMed: 31918004]
- Noor S, Sanchez JJ, Vanderwall AG, Sun MS, Maxwell JR, Davies S, Jantzie LL, Petersen TR, Savage DD, and Milligan ED. 2017. 'Prenatal alcohol exposure potentiates chronic neuropathic pain, spinal glial and immune cell activation and alters sciatic nerve and DRG cytokine levels', *Brain, behavior, and immunity*, 61: 80–95. [PubMed: 28011263]
- Noor S, Sun MS, Vanderwall AG, Havard MA, Sanchez JE, Harris NW, Nysus MV, Norenberg JP, West HT, Wagner CR, Jantzie LL, Mellios N, and Milligan ED. 2019. 'LFA-1 antagonist (BIRT377) similarly reverses peripheral neuropathic pain in male and female mice with underlying sex divergent peripheral immune proinflammatory phenotypes', *Neuroimmunol Neuroinflamm*, 6: 1–32.
- O'Neill LA, and Bowie AG. 2007. 'The family of five: TIR-domain-containing adaptors in Toll-like receptor signalling', *Nat Rev Immunol*, 7: 353–64. [PubMed: 17457343]
- Ozaktay AC, Kallakuri S, Takabayashi T, Cavanaugh JM, Asik I, Deleo JA, and Weinstein JN. 2006. 'Effects of interleukin-1 beta, interleukin-6, and tumor necrosis factor on sensitivity of dorsal root ganglion and peripheral receptive fields in rats', *Eur Spine J*: 58–66.
- Rangel-Barajas C, Coronel I, and Floran B. 2015. 'Dopamine Receptors and Neurodegeneration', *Aging Dis*, 6: 349–68. [PubMed: 26425390]

- Robinson I, and Meert TF. 2005. 'Stability of neuropathic pain symptoms in partial sciatic nerve ligation in rats is affected by suture material', *Neuroscience letters*, 373: 125–9. [PubMed: 15567566]
- Rodgers HM, Yow J, Evans E, Clemens S, and Brewer KL. 2019. 'Dopamine D1 and D3 receptor modulators restore morphine analgesia and prevent opioid preference in a model of neuropathic pain', *Neuroscience*, 406: 376–88. [PubMed: 30910641]
- Ruohonen S, Jagodi M, Khademi M, Taskinen HS, Ojala P, Olsson T, and Roytta M. 2002. 'Contralateral non-operated nerve to transected rat sciatic nerve shows increased expression of IL-1beta, TGF-beta1, TNF-alpha, and IL-10', *Journal of Neuroimmunology*, 132: 11–7. [PubMed: 12417428]
- Sadeghi H, Parishani M, Akbartabar Touri M, Ghavamzadeh M, Jafari Barmak M, Zarezade V, Delaviz H, and Sadeghi H. 2017. 'Pramipexole reduces inflammation in the experimental animal models of inflammation', *Immunopharmacol Immunotoxicol*, 39: 80–86. [PubMed: 28162057]
- Samad TA, Wang H, Broom DC, and Woolf CJ. 2004. "Central neuroimmune interactions after peripheral inflammation: interleukin-1b potentiates synaptic transmission in the spinal cord." In *Proc Soc Neurosci*, 511.7.
- Sanchez JJ, Noor S, Davies S, Savage D, and Milligan ED. 2017. 'Prenatal alcohol exposure is a risk factor for adult neuropathic pain via aberrant neuroimmune function', *J Neuroinflammation*, 14: 254. [PubMed: 29258553]
- Santamaria-Anzures J, Perez-Ramos J, Mendoza-Perez F, and Godinez-Chaparro B. 2023. 'Pramipexole inhibits formalin-Induce acute and long-lasting mechanical hypersensitivity via NF-kB pathway in rats', *Drug Dev Res*.
- Schneider CS, and Mierau J. 1987. 'Dopamine autoreceptor agonists: resolution and pharmacological activity of 2,6-diaminotetrahydrobenzothiazole and an aminothiazole analogue of apomorphine', *J Med Chem*, 30: 494–8. [PubMed: 3820220]
- Schreiber KL, Beitz AJ, and Wilcox GL. 2008. 'Activation of spinal microglia in a murine model of peripheral inflammation-induced, long-lasting contralateral allodynia', *Neurosci Lett*, 440: 63–7. [PubMed: 18541374]
- Sibley DR, Monsma FJ Jr., and Shen Y. 1993. 'Molecular neurobiology of dopaminergic receptors', *Int Rev Neurobiol*, 35: 391–415. [PubMed: 8463063]
- Sideris-Lampretsas G, and Malcangio M. 2021. 'Microglial heterogeneity in chronic pain', *Brain, behavior, and immunity*, 96: 279–89. [PubMed: 34139287]
- Sloane EM, Langer SJ, Milligan ED, Weiseler-Frank J, Mahoney JH, Levkoff L, Chavez RA, Cruz PE, Flotte TR, Leinwand LA, Maier SF, and Watkins LR. 2004. "Chronic Constriction Injury induced pathological pain states are controlled long term via intrathecal administration of a non-viral vector(NVV) encoding the anti-inflammatory cytokine interleukin-10 (IL-10)." In *2nd Joint Scientific Meeting of the American PAin Society & the Canadian Pain Society*, edited by Gebhart GF, 15. Churchill Livingstone.
- Sommer C, and Schafers M. 1998. 'Painful mononeuropathy in C57BL/Wld mice with delayed wallerian degeneration: differential effects of cytokine production and nerve regeneration on thermal and mechanical hypersensitivity', *Brain research*, 784: 154–62. [PubMed: 9518588]
- Sorge RE, Mapplebeck JC, Rosen S, Beggs S, Taves S, Alexander JK, Martin LJ, Austin JS, Sotocinal SG, Chen D, Yang M, Shi XQ, Huang H, Pillon NJ, Bilan PJ, Tu Y, Klip A, Ji RR, Zhang J, Salter MW, and Mogil JS. 2015. 'Different immune cells mediate mechanical pain hypersensitivity in male and female mice', *Nature neuroscience*, 18: 1081–3. [PubMed: 26120961]
- Tamae A, Nakatsuka T, Koga K, Kato G, Furue H, Katafuchi T, and Yoshimura M. 2005. 'Direct inhibition of substantia gelatinosa neurones in the rat spinal cord by activation of dopamine D2-like receptors', *J Physiol*, 568: 243–53. [PubMed: 15975975]
- Urru M, Muzzi M, Coppi E, Ranieri G, Buonvicino D, Camaioni E, Coppini R, Pugliese AM, Tanaka B, Estacion M, Waxman SG, Dib-Hajj SD, and Chiarugi A. 2020. 'Dexpramipexole blocks Nav1.8 sodium channels and provides analgesia in multiple nociceptive and neuropathic pain models', *Pain*, 161: 831–41. [PubMed: 31815915]
- Vanderwall AG, Noor S, Sun MS, Sanchez JE, Yang XO, Jantzie LL, Mellios N, and Milligan ED. 2017. 'Effects of spinal non-viral interleukin-10 gene therapy formulated with D-mannose in

neuropathic interleukin-10 deficient mice: behavioral characterization, mRNA and protein analysis in pain relevant tissues', *Brain, behavior, and immunity*.

- . 2018. 'Effects of spinal non-viral interleukin-10 gene therapy formulated with d-mannose in neuropathic interleukin-10 deficient mice: Behavioral characterization, mRNA and protein analysis in pain relevant tissues', *Brain, behavior, and immunity*, 69: 91–112. [PubMed: 29113923]
- Vellucci R 2012. 'Heterogeneity of chronic pain', *Clin Drug Investig*, 32 Suppl 1: 3–10.
- Viviani B, Bartesaghi S, Gardoni F, Vezzani A, Behrens MM, Bartfai T, Binaglia M, Corsini E, DiLuca M, Galli CL, and Marinovich M. 2003. 'Interleukin-1beta enhances NMDA receptor-mediated intracellular calcium release through activation of the Src family of kinases', *J Neurosci*, 23: 8692–700. [PubMed: 14507968]
- Watkins LR, Hutchinson MR, Rice KC, and Maier SF. 2009. 'The "toll" of opioid-induced glial activation: improving the clinical efficacy of opioids by targeting glia', *Trends Pharmacol Sci*, 30: 581–91. [PubMed: 19762094]
- Waxman SG, and Zamponi GW. 2014. 'Regulating excitability of peripheral afferents: emerging ion channel targets', *Nature neuroscience*, 17: 153–63. [PubMed: 24473263]
- Wei MT, Hua KF, Hsu J, Karmenyan A, Tseng KY, Wong CH, Hsu HY, and Chiou A. 2007. 'The interaction of lipopolysaccharide with membrane receptors on macrophages pretreated with extract of Reishi polysaccharides measured by optical tweezers', *Opt Express*, 15: 11020–32. [PubMed: 19547459]
- Wieseler-Frank J, Kwicien O, Jekich B, Maier SF, and Watkins LR. 2004. "Putative neuron-to-glia signals synergize to enhance interleukin-1 production by rat dorsal spinal cord glial cells in vitro." In *Soc for Neurosci Abstr*.
- Wilkerson JL, Alberti LB, Kerwin AA, Ledent CA, Thakur GA, Makriyannis A, and Milligan ED. 2020. 'Peripheral versus central mechanisms of the cannabinoid type 2 receptor agonist AM1710 in a mouse model of neuropathic pain', *Brain and behavior*, 10: e01850. [PubMed: 32977358]
- Wilkerson JL, Alberti LB, Thakur GA, Makriyannis A, and Milligan ED. 2022. 'Peripherally administered cannabinoid receptor 2 (CB2R) agonists lose anti-allodynic effects in TRPV1 knockout mice, while intrathecal administration leads to anti-allodynia and reduced GFAP, CCL2 and TRPV1 expression in the dorsal spinal cord and DRG', *Brain research*, 1774: 147721. [PubMed: 34774500]
- Wilson SM, Wurst MG, Whatley MF, and Daniels RN. 2020. 'Classics in Chemical Neuroscience: Pramipexole', *ACS Chem Neurosci*, 11: 2506–12. [PubMed: 32786316]
- Woller SA, Ravula SB, Tucci FC, Beaton G, Corr M, Isseroff RR, Soulika AM, Chigbrow M, Eddinger KA, and Yaksh TL. 2016. 'Systemic TAK-242 prevents intrathecal LPS evoked hyperalgesia in male, but not female mice and prevents delayed allodynia following intraplantar formalin in both male and female mice: The role of TLR4 in the evolution of a persistent pain state', *Brain, behavior, and immunity*, 56: 271–80. [PubMed: 27044335]
- Zhu H, Clemens S, Sawchuk M, and Hochman S. 2007. 'Expression and distribution of all dopamine receptor subtypes (D(1)-D(5)) in the mouse lumbar spinal cord: a real-time polymerase chain reaction and non-autoradiographic in situ hybridization study', *Neuroscience*, 149: 885–97. [PubMed: 17936519]
- Zhu J, Hu Z, Han X, Wang D, Jiang Q, Ding J, Xiao M, Wang C, Lu M, and Hu G. 2018. 'Dopamine D2 receptor restricts astrocytic NLRP3 inflammasome activation via enhancing the interaction of beta-arrestin2 and NLRP3', *Cell Death Differ*, 25: 2037–49. [PubMed: 29786071]

### Highlights

- Pramipexole and dexpramipexole are anti-inflammatory agents and induce anti-allodynia
- Pramipexole directly blunts IL-1 $\beta$  protein levels in human stimulated monocytes
- Dexpramipexole increases IL-10 production in stimulated peripheral leukocytes

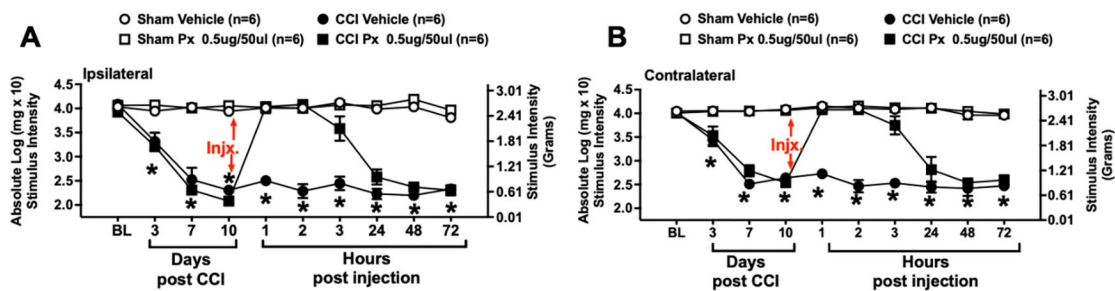


**Figure 1: Injection of pramipexole (Px) fully reverses CCI-induced hindpaw allodynia in mice.** Behavioral responses to light touch stimuli applied to the plantar surface of the hindpaw ipsilateral (A) and contralateral (B) to sciatic nerve chronic constriction injury (CCI) reveal that stimulus thresholds of mice at baseline (BL) are similar between all groups. Following sciatic nerve manipulation, sham treatment results in bilaterally stable non-sensitized hindpaw responses, while CCI induces robust development of bilateral allodynia that peaks by Day 10. After behavioral assessment of all mice on Day 10, mice received intravenous (i.v.) 0.5 ug pramipexole (Px), or equivolume vehicle. Px given to sham-treated mice does not alter hindpaw thresholds throughout the remainder of the timecourse, demonstrating that Px, per se, does not impact normal sensory thresholds under non-pathological conditions. Px transiently reverses bilateral allodynia compared to vehicle-injected CCI-treated mice. Maximal bilateral reversal from allodynia is observed from 1–3 hrs, with bilateral allodynia returning by 24 hrs and remaining stable through 72 hrs after injection. Each timepoint marked with \* indicates *post-hoc* analysis confirming that mice with CCI and treated with vehicle of Px remained robustly allodynic compared to sham given vehicle or Px, and CCI mice treated with Px. \* =  $p < 0.0001$

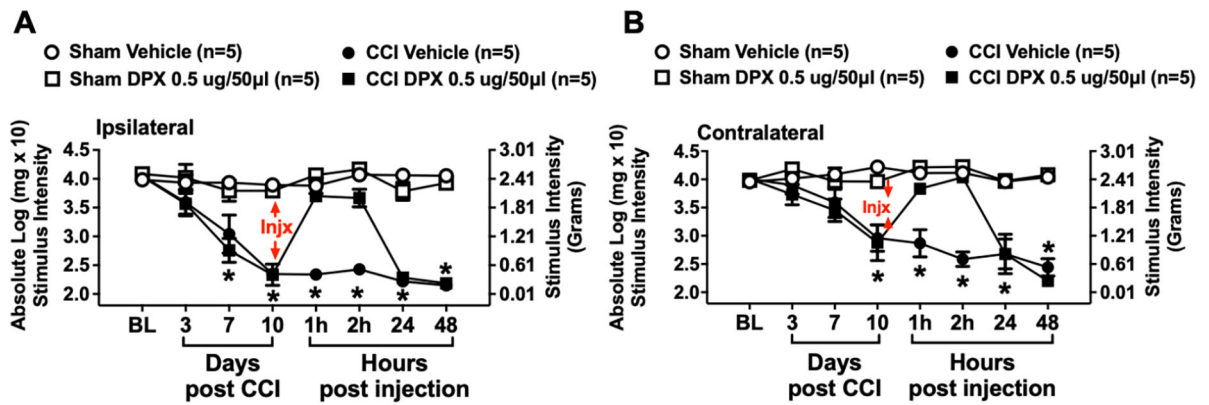


**Figure 2: Injection of dexpramipexole (DPX) fully reverses CCI-induced hindpaw allodynia in mice.**

Dexpramipexole (DPX) is the stereoisomer of Px, and is functionally distinguishable from Px due to DPX's weak action at dopamine D2/D3 receptors. Behavioral responses to light touch stimuli applied to the plantar surface of the hindpaw ipsilateral (**A**) and contralateral (**B**) to sham or sciatic nerve chronic constriction injury (CCI) reveal that hindpaw responses of mice at BL are similar between all groups. Following sciatic nerve manipulation, sham-treated mice reveal bilaterally stable non-sensitized hindpaw responses, while unilateral CCI induces robust development of bilateral allodynia, again peaking by Day 10 after CCI. After behavioral assessment of all mice on Day 10, hindpaw thresholds of sham-treated mice given either i.v. 0.5 ug DPX or equivolume vehicle remained stable and bilaterally responsive but non-allodynic throughout the remainder of the timecourse. However, mice treated with i.v. 0.5 ug DPX revealed a complete reversal of allodynia, with maximal effects again observed at 1 and 2 hrs after injection, with allodynia returning 24 hrs later and remaining stable through 48 hrs. Mice receiving intravenous (i.v.) equivolume vehicle remained bilaterally stably allodynic throughout the timecourse. Each timepoint marked with \* indicates posthoc analysis confirming that mice with CCI and treated with vehicle of DPX remained robustly allodynic compared to sham given vehicle or Px, and CCI mice treated with DPX. \* =  $p < 0.0001$



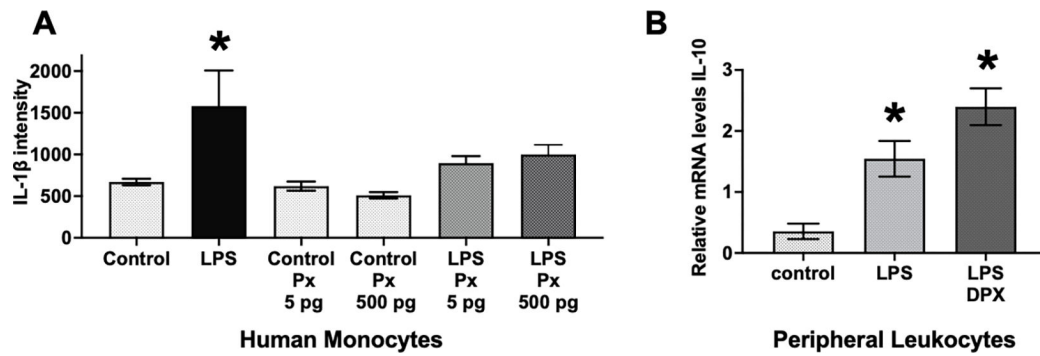


**Figure 3: Pramipexole (Px) treatment suppresses IL-1 $\beta$  release and dexpramipexole (DPX) enhances IL-10 mRNA transcription in LPS stimulated human monocytes and peripheral immune cells.**

(A) Under cell culture conditions using an undifferentiated human monocyte cell line, THP-1 cells, pramipexole is capable of suppressing protein levels of the pro-nociceptive cytokine, interleukin-1beta (IL-1 $\beta$ ), from being released after classic immune cell stimulation with the gram-negative bacteria cell wall particles, lipopolysaccharide (LPS). Pramipexole (5 pg and 500 pg) does not significantly alter basal cellular levels of IL-1 $\beta$ . However, both 5 pg and 500 pg of pramipexole in the presence of LPS stimulation significantly blunts IL-1 $\beta$  protein release. (B) DPX significantly increased mRNA levels of the anti-inflammatory cytokine, IL-10. Under cell culture conditions of isolated peripheral immune splenocytes, LPS significantly elevated IL-10 mRNA compared to untreated cells. LPS + DPX treatment further elevated IL-10 mRNA compared to LPS only treatment. For panels A and B, \* =  $P < 0.001$ .